Macromolecular Research, Vol. 23, No. 12, pp 1091-1097 (2015)
DOI 10.1007/s13233-015-3156-4

www.springer.com/13233
pISSN 1598-5032 eISSN 2092-7673

Effect of Pore Sizes of Silk Scaffolds for Cartilage Tissue Engineering

Kap-Soo Han[†,1], Jeong Eun Song[†,2], Nirmalya Tripathy[2], Hyeongseok Kim[2], Bo Mi Moon[3], Chan Hum Park[3], and Gilson Khang[*,2]

[1]*School of Medicine, Chonbuk National Univ. Medical School, 20 Gungiro, Jeonju 561-756, Korea*
[2]*Department of BIN Fusion Tech., Polymer Fusion Res. Center & Dept. of Polymer·Nano Sci Tech, Chonbuk National Univ., 567 Baekje-daero, Jeonju 561-756, Korea*
[3]*Nano-Bio Regenerative Medical Institute, Hallym University, Okcheon-dong 1, Chuncheon 200-702, Korea*

Received March 2, 2015; Revised October 6, 2015; Accepted October 11, 2015

Abstract: The aim of this study was to investigate the effects of silk fibroin scaffold, a natural biodegradable polymer scaffold, on the adhesive and proliferative behaviors of chondrocytes. Various silk fibroin scaffolds were produced using the salt extraction method, and scaffolds with different pore sizes (90-180, 180-250, 250-355, and 355-425 μm) were constructed based on the size of the salt particles. Chondrocytes were seeded on the scaffolds and incubated. The produced scaffolds were analyzed with Fourier transform-infrared spectroscopy and exhibited characteristics similar to those of natural silk in terms of chemical composition and structure. Moreover, we found that the mechanical strength decreased as the pore size increased. Scanning electron microscopy images confirmed the existence of pores in the silk fibroin scaffold. Additionally, scaffolds with smaller pore sizes facilitated improved cell adhesion. Using MTT analysis, we found that scaffold with pore sizes of 90-180 and 180-250 μm provided the best environment for cell proliferation. The amount levels of sulfated glycosaminoglycan (sGAG) and collagen were highest for scaffolds with a pore size of 90-180 μm. In gene expression analysis, scaffolds with pore sizes of 90-180 and 180-250 μm showed the highest expression of the chondrocytes marker aggrecan and type II collagen. Collectively, these data suggest that silk fibroin scaffolds with smaller pore sizes (90-250 μm) provide the best environment for adhesion and proliferation of chondrocytes.

Keywords: chondrocytes, silk fibroin, pore, scaffold, cartilage regeneration.

Introduction

Tissue engineering, a major focus of life sciences and engineering technologies, may allow cells and tissues transplanted into human organs to maintain, restore, or enhance organ function.[1-4] Recently, great progress has been made in tissue engineering-related biomaterials, drug delivery systems, stem cell research, and nanotechnology. Thus, tissue engineering applications have expanded to use in the clinical setting and in regenerative medicine.[5-7]

A proper scaffold is critical for providing a stable environment on which cells can regenerate into useful tissues for tissue engineering applications.[8,9] The three-dimensional porous structure of the scaffold provides an environment on which the seeded cells can move to adjacent areas, proliferate, and differentiate into various tissues.[10-12] Additionally, the scaffold should provide an environment with appropriate nutrients and oxygen for regeneration of cells and tissues into similar adjacent tissues. Therefore, to produce proper scaffolds, the process of investigating the physical characteristics such as pore size, water absorption ability and morphology should be performed.[13,14]

Various scaffold structures such as foams, fibers, and microspheres are used as a matrix for cell seeding and culture.[15] Natural polymers have been widely used for tissue engineering materials due to their rapid biodegradable aspect.[16-20] Recently, silk is widely used as the material for the scaffolds.[21,22] Silk from silkworm (*Bombyx mori*) is comprised of 75% fibroin and 25% sericin and carbohydrates, with an amino acid composition similar to collagen. Silk is commonly used for surgical sutures with removal of sericin.[23] Due to its high biocompatibility, silk can be used as a scaffold to promote the growth of mesenchymal stem cells, epithelial cells, fibroblasts, and keratinocytes.[24] Moreover, silk is known to decompose within 6 months in the body, lose its tensile strength within 1 year, and completely decompose within 2 years. Therefore, silk may represent a promising biomaterial for scaffolding in tissue engineering applications.

Cartilage tissue has a unique structure consisting of low

*Corresponding Author. E-mail: gskhang@jbnu.ac.kr
[†]These authors equally contributed to this work.

density of chondrocytes and extracellular matrix. Since cartilage tissue does not have blood vessels, nerves, or lymphatic vessels, regeneration of injured cartilage tissue is limited.[25-27] An ideal scaffold for cartilage tissue engineering should contain the following characteristics including biocompatible, biodegradable, highly porous, promoting cell attachment and proliferation.[28] Importantly, pore size of scaffold is crucial to provide good environment for cells growth. It was reported that cell migration, delivery and spatial distribution could be limited in case of too small sized pores because of the systems for nutrients diffusion and removal of waste from the cells couldn't be facilitated within the scaffold structure. On the contrary, in case of too large sized pores, cell growth is also decreased due to the limited surface for cell adhesion.[29,30]

In this study, we investigated the optimum pore size of the scaffold required for cartilage tissue engineering. The silk fibroin scaffolds with various pore sizes (*i.e.* 90-180, 180-250, 250- 355, and 355-425 μm) were fabricated *via* silk aqueous solution through salt extraction method. Then, scaffold's physiochemical, mechanical properties, and cell attachment, proliferation and growth efficiency of cartilage chondrocytes within the scaffolds were assessed.

Experimental

Reagents and Materials. Silk was obtained from the Rural Development Administration (Korea) and LiBr was purchased from Kanto Chemical (Japan). Dialyzing diaphragm (Snakeskin™ Dialysis Tubing, MWCO 3,500) was bought from Thermo scientific (USA). Sodium chloride and methylene chloride were purchased from SHOWA Chemical (Japan) and Samchun Pure Chemical Co., Ltd (Korea), respectively. All reagents in this experiment were remarked a high performance liquid chromatography (HPLC) grade.

Preparation of Silk Fibroin Solution. In order to prepare silk fibroin solution, sericin in cocoon was removed and boiled in 0.02 M of Na_2CO_3 solution for an hour to obtain pure fibroin. After an hour of boiling, the silk fibroin was washed with distilled water three times and dried for three days in room temperature. Dried silk fibroin was immersed in 9.3 M LiBr solution and was melted under 60 °C of temperature in the oven for 4 h. LiBr was dialyzed from the silk fibroin solution using dialyzing diaphragm (SnakeSkin™ Dialysis Tubing, MWCO 3,500) for three days and the distilled water was changed in the order of 1, 4, 8, 12, 12, 12, 12 h. Remained impurities were removed from silk fibroin solution after dialyzing and the solution were kept under 4 °C of temperature in the refrigerator.

Fabrication of Various Silk Fibroin Scaffolds. Silk fibroin scaffold with various pore sizes were prepared using salt leaching method. Obtained silk fibroin solution and NaCl were mixed at 1:2 mass ratio in the rubber mold and dried in the room temperature for five days. The pore size of silk fibroin was determined by the size of the salt: 90-180, 180-250, 250-355, and 355-425 μm. The silk fibroin scaffold was immersed in the methanol for an hour to crystalize. Afterward, crystalized silk fibroin scaffold were also immersed in the distilled water to remove the salt and the distilled water was changed every 6 h. Scaffolds were finally lyophilized at -80 °C and 5 mTorr for 24 h using a freeze dryer (Model FDU-540, EYELA, Japan). Dried silk fibroin scaffold were used after sterilizing in 70% of alcohol.

Mechanical and Chemical Analysis of Scaffolds. FTIR (fourier transformed-intrared) analysis, compressive strength measurement and swelling test were performed to measure the mechanical and chemical characteristics of scaffolds. FTIR-300E Spectrometer (JASCO, Japan) was used to analyze the chemical property of prepared scaffolds. First, the test was conducted without any scaffold and was set as control to compare with scaffolds which contains silk fibroin at the pore size of 90-180, 180-250, 250-355, and 355-425 μm, respectively. The measurement range was 4000~650 cm^{-1} and the resolution was 8 cm^{-1}. Compressive strength of each scaffold was measured using texture analyzer (TMS-Pro, Sterling, VA, USA). To calculate the strength, the height of scaffold was measured and the scaffold was moved down at the speed of 20 mm/s and the force of 0.5 N until the scaffold was pressed down to reach half its height. The weight of each scaffold was measured and the swelling ratio of each scaffold was evaluated by immersing dried scaffold into the distilled water with the same weight of scaffold. The total weight of immersed scaffold was measured and the ratio was calculated by subtracting the weight of dried scaffold from the total weight.

SEM Image for Morphological Characterization. The morphology of silk fibroin scaffold and its adhesion and proliferation of seeded cells according to the pore size was observed using SEM (S-2250 N, Hitachi, Tokyo, Japan). The chondrocytes were seeded and cultured for 21 days. After culturing, the culture medium was removed and the scaffold was washed with phosphate-buffered saline (PBS, Gibco) and was fixed with 2.5% glutaraldehyde (Sigma) in PBS for 24 h at room temperature. Then the scaffold was dehydrated for 30 min with using a graded series of ethanol (50, 60, 70, 80, 90, and 100%) and completely dried. The samples was prepared by cross sectioning of the scaffolds and fixed on slides. Adhered cells and scaffolds were coated with white gold of 200 μm in thickness using a plasma sputter (Emscope SC500K, London, UK) under argon gas. The morphology of silk fibroin scaffold was observed using a SEM at 20 kV.

Cell Proliferation. MTT (3-[4, 5-dimethylthiazol-2-yl]-2, 5-diphenyl tetrazolium bromide, Sigma, USA) analysis was carried out for the observation of adhesion and proliferation on the scaffold. The chondrocytes were seeded on the prepared scaffold and after 1, 3, 5, 7, 10, and 14 days, 100 μL of MTT solution was added and incubated for 4 h at 37 °C with 0.5% of CO_2. After incubation, when purple crystals were observed, the media and MTT solution were completely removed. The scaffold was carefully washed with PBS and

incubated with the addition of 1 mL of dimethyl sulfoxide (Sigma) for 24 h. The solution (100 μL) was pipetted into a 96-well plate, and the absorbance at 570 nm was measured with ELISA plate-reader (BioTek, USA).

sGAG and Collagen Content Measurement. After chondrocytes were seeded depending on the pore size in 1, 2, and 3 weeks scaffolds were frozen and finally lyophilized at -70 °C and 5 mTorr. 1 mL of papain solution (125 μg/mL of papain, 5 mM of L-cysteine, 100 mM of Na_2HPO_4, 5 mM of EDTA, pH 6.8) were added to prepared scaffold and activated for 16 h at 60°C. sGAG contents in scaffolds were measured using a 1,9 dimethylene blue (DMMB) dye-binding technique. 500 μL of papain added solution was mixed with 500 μL of DMMB solution and stirred for 20 min at room temperature. The solution (100 μL) was pipetted into a 96-well plate, and the absorbance at 570 nm was measured with ELISA plate-reader (BioTek, USA). Total amount of sGAG was calculated based on chondroitin sulfate (Sigma). To measure the produced collagen, 900 μL of 6 N HCl was added to the prepared solution and heated in an oil bath at 107 °C for 16 h. Chloramine-T (0.56 M) solution was diluted with distilled water at 1:1 ratio and diluted chloramine solution was mixed with acetate citrate buffer solution (6 g of sodium acetate trihydrate, 2.3 g of citric acid, 1.7 g of sodium hydroxide (NaOH), 0.6 mL of acetic acid, 49.4 mL of distilled water) at 1:5 ratio. 50 μL of the boiled solution sample was taken and mixed with 50 μL of NaOH (4 M) and 50 μL of mixed solution was removed. 450 μL of chloramine-T solution was added to the solution sample and stirred for 25 min. 500 μL of Ehrlich aldehyde solution was added and activated in the oven at 65 °C for 20 min. 100 μL of solution was pipetted into a 96-well plate, and the absorbance at 570 nm was measured with ELISA plate-reader (BioTek, USA). Total amount of collagen was calculated by measuring hydroxyproline (Sigma).

Reverse Transcription-Polymerase Chain Reaction (RT-PCR) Analysis. RT-PCR analysis was performed to confirm RNA expression and determine the effect of the pore size of silk fibroin scaffold. The prepared silk fibroin scaffold was placed in 24-well plate and was sterilized in 70% of alcohol. 1×10^5 chondrocytes were seeded on the scaffolds and cultured for 7, 14, and 21 days. The medium was removed and 1 mL of trizol (TaKaRa) was added to the scaffold, which was then centrifuged at 12,000×g for 10 min at 4 °C. RNA was extracted by mixing with 0.5 mL of isopropanol (Sigma-Aldrich) and 5 μL of Polyacryl Carrier™ (Molecular Research Center, Inc.). The extracted RNA, β-actin, aggrecan, type II and I collagen were transcribed with One-step RT PCR DryMix (Enzynomics). Amplified DNA after PCR was added into 1.5% (w/v) agarose gel (Sigma) and electrophoresis was conducted at 100 V for 25 min. Relative expression was analyzed with SYBR Green PCR (SYBRTM Green I Nucleic Acid Gel Stain, Cambrex, U.K). The presence of bands was observed using an ultraviolet transilluminator (Vilber Lourmat ETX-20.M; France). The expression levels were measured using Image J and normalized to β-actin.

Histological Evaluation Analysis. To perform immunohistochemical analysis according to the pore size of silk fibroin scaffolds, 1×10^5 chondrocytes were seeded on the scaffolds. The cell-seeded scaffolds were implanted into the subcutaneous region of nude mouse (1, 3, and 5 weeks). All experiments were carried out according to the institutional guidelines for care and use of laboratory animals. The silk fibroin scaffolds were extracted at (1, 3, and 5 weeks). and fixed in the formalin solution (10%). Paraffin sections were cut to be 4 μm thickness using microtome (Thermo Scientific). Hematoxylin and eosin (H&E) staining was used to analyze the cell proliferation and alcian blue staining for cartilage matrix.

Statistical Analysis. Data are presented as mean ± standard deviation (SD). Statistical analysis was conducted based on Student's *t*-test (Excel2007, Microsoft) and the differences were considered significant at $p < 0.05$ (*).

Results and Discussion

Fourier-Transform Infrared Spectroscopy (FTIR) of Scaffold. FTIR was performed to analyze the chemical compositions of silk fibroin scaffolds (Figure 1). We assume that change in the scaffold's pore sizes would not change its chemical composition, thus we analyzed FTIR for silk fibroin scaffolds with 90-180 μm. The as-fabricated scaffolds showed amide groups forming β-sheet structure at 1630 (amide I), 1530 (amide II), and 1265 (amide III) cm^{-1}, confirming that the scaffolds didn't lose the properties of silk during production process.[31]

Compressive Strength of the Scaffolds. Compressive strength was measured in silk fibroin scaffolds with different pore sizes to evaluate the mechanical properties of the scaffolds (Figure 2). Compared to 90-180, 180-250, 250-355, and 355-425 μm scaffolds showed no significant differences in statistical analysis. Compressive strength in native cartilage tissue was measured 0.1-1 MPa.[32] The highest strength among the scaffolds was found in scaffolds with 90-180 μm pores. As the size of the pores increased, the strength of the silk scaf-

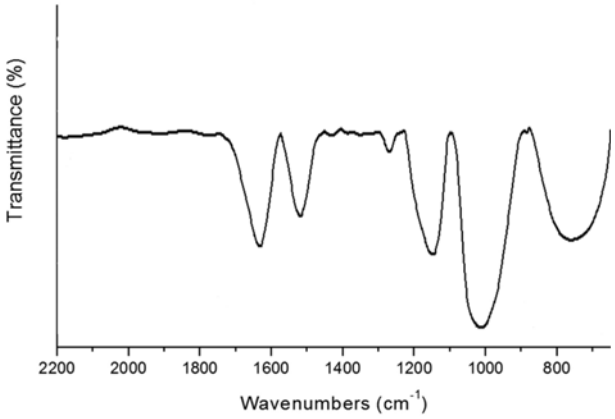

Figure 1. FTIR of silk fibroin scaffold with 90-180 μm pore size.

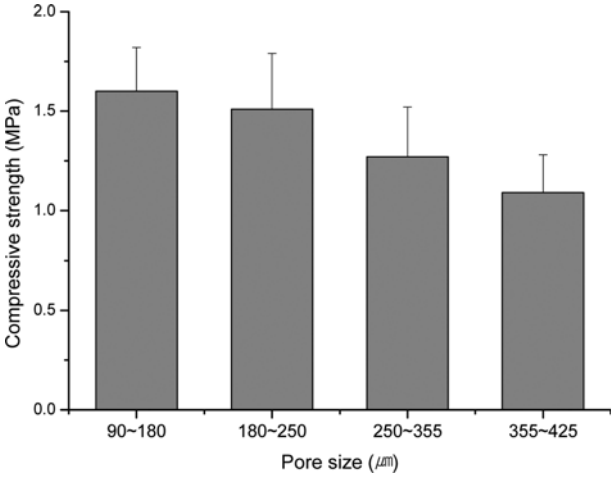

Figure 2. Compressive strength of silk fibroin scaffolds with various pore sizes.

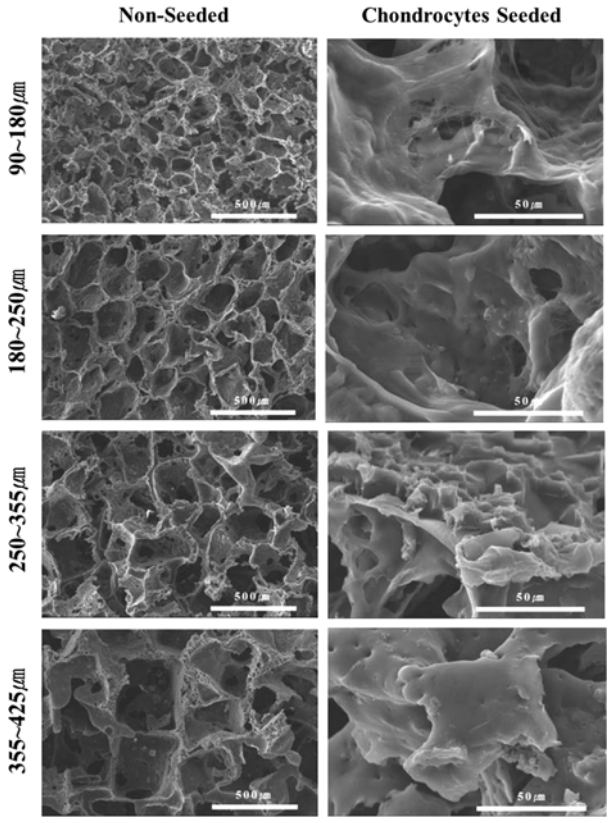

Figure 3. SEM images of silk fibroin scaffolds and cells on the scaffolds (Scale bar = 500 μm, 50 μm).

fold decreased. Compression strengths were 1.6, 1.51, 1.27, and 1.09 MPa for scaffolds with pore sizes of 90-180, 180-250, 250-355, and 355-425 μm, respectively. This result was expected since denser structure of the least pore size scaffold can withstand the higher loads than others.

Scanning Electron Microscope. Figure 3 shows the average pore sizes of scaffolds studied using Image J. Results

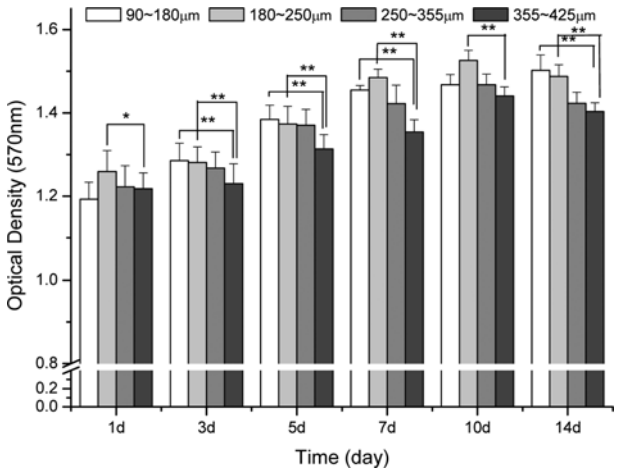

Figure 4. Cell viability of chondrocytes on silk fibroin scaffold with various pore sizes for 1, 3, 5, 7, 10, and 14 days (**p<0.01, *p<0.05).

showed that the scaffolds with 90-180, 180-250, 250-355, and 355-425 μm pore possess measured pore size of 127.78±51.03, 215.14±49.31, 285.61±45.04, and 373.25±77.10 μm, respectively. Moreover, the inter-pores between the pores were also measured. The scaffolds with 90-180, 180-250, 250-355, and 355-425 μm pores size demonstrated 18±7.04, 25±10.09, 28.37±14.5, and 32.16±18.06 μm, respectively.

MTT Analysis. Then, chondrocytes were seeded on silk fibroin scaffolds having various pore sizes, and cell growth was observed for 21 days. MTT analysis of cartilage cell proliferation on the silk fibroin scaffold is shown in Figure 4. After 1 day of culture, cells exhibited the highest proliferation rate on scaffolds with pore sizes of 180-250 μm, while after 3 days culture, cells grown on scaffolds with pore sizes of 90-180 μm exhibited the highest proliferation rates. Thus, the cells and extracellular matrix were well-attached and proliferated effectively on scaffolds with pore sizes of 90-180 and 180-250 μm. Further, reduced cell proliferation was observed for cells grown on scaffolds with pore sizes of 250-355 and 355-425 μm. Thus, these data supported that cells attached and proliferated better on scaffolds with smaller pore sizes (90-250 μm) than on scaffolds with larger pore sizes. And, scaffolds with certain pore sizes were not suitable for cell attachment and expansion to adjacent structures.

Sulfated Glycosaminoglycan (sGAG) and Collagen Contents. Figure 5 shows the sGAG and collagen contents in the silk fibroin scaffolds. Generally, sGAG contents increased in all scaffolds after 1-2 weeks and began to decrease after 2 weeks. sGAG contents were highest for scaffold with 90-180 μm pores at week 1 and were high for scaffolds with 90-180 and 180-250 μm pores at week 2. sGAG content decreased slightly during week 3; however, sGAG contents in scaffolds with pores of 90-180 and 180-250 μm continued to measure higher than those in scaffolds with larger pores. A similar trend was observed for collagen contents, with highest expression levels observed

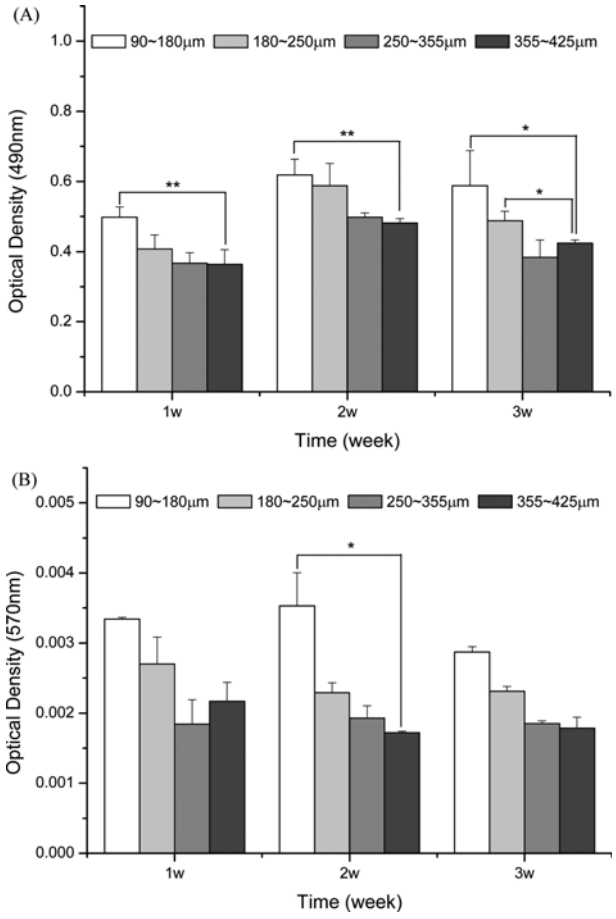

Figure 5. sGAG and collagen content of chondrocytes seeded silk fibroin scaffolds for 1, 2, and 3 weeks. (A) sGAG and (B) collagen content (**p<0.01, *p<0.05).

for scaffolds with 90-180 μm pores at week 1, followed by a slight decrease in collagen contents during weeks 2 and 3. Additionally, collagen contents decreased with increasing pore sizes. Therefore, these data demonstrated that scaffolds with smaller pores, which also exhibited improved cell attachment and proliferation, had increased sGAG and collagen contents.

Analysis of Gene Expression by Reverse Transcription Polymerase Chain Reaction (RT-PCR). Next, we analyzed gene expression levels in chondrocytes grown on silk fibroin scaffolds using RT-PCR (Figure 6). At week 1, aggrecan, a marker of chondrocytes, exhibited the highest expression in scaffolds with 180-250 μm pores and the lowest expression in scaffolds with 355-425 μm pores (the largest pore size examined in this study. However, by week 2, the expression of aggrecan increased in scaffolds with 90-180 μm pores, surpassing the expression levels observed in scaffolds with 180-250 μm pores (although the difference was not statistically significant. The expression of aggrecan tended to decrease during week 3, consistent with the occurrence of cell death beginning at this time point. Moreover, as pore size increased, expression of aggrecan decreased. Similar trends were observed for the

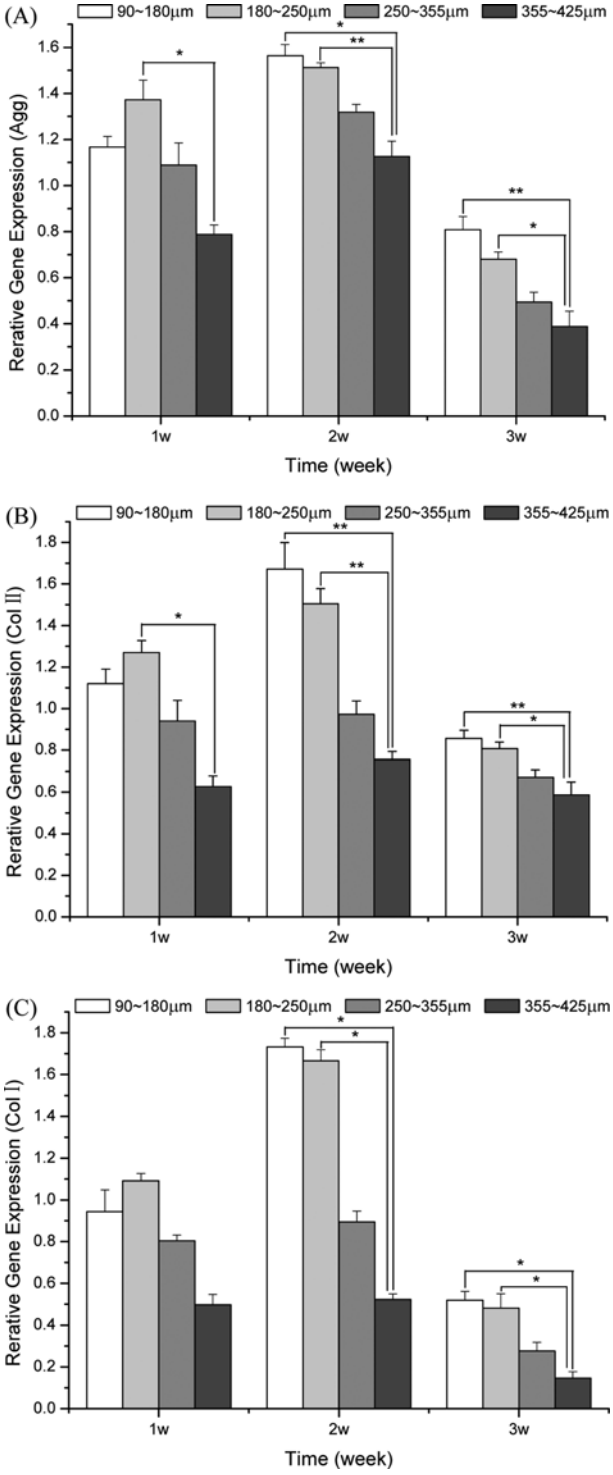

Figure 6. Gene expression of chondrocytes on silk fibroin scaffolds as analyzed by RT-PCR at 1, 2, and 3 weeks. (A) Aggrecan, (B) type II collagen, and (C) type I collagen (**p<0.01, *p<0.05).

expression of type II collagen and type I collagen, with the highest expression levels observed in scaffolds having 90-250 μm pores. Interestingly, for type I collagen, expression levels decreased more dramatically, reaching only two-thirds the

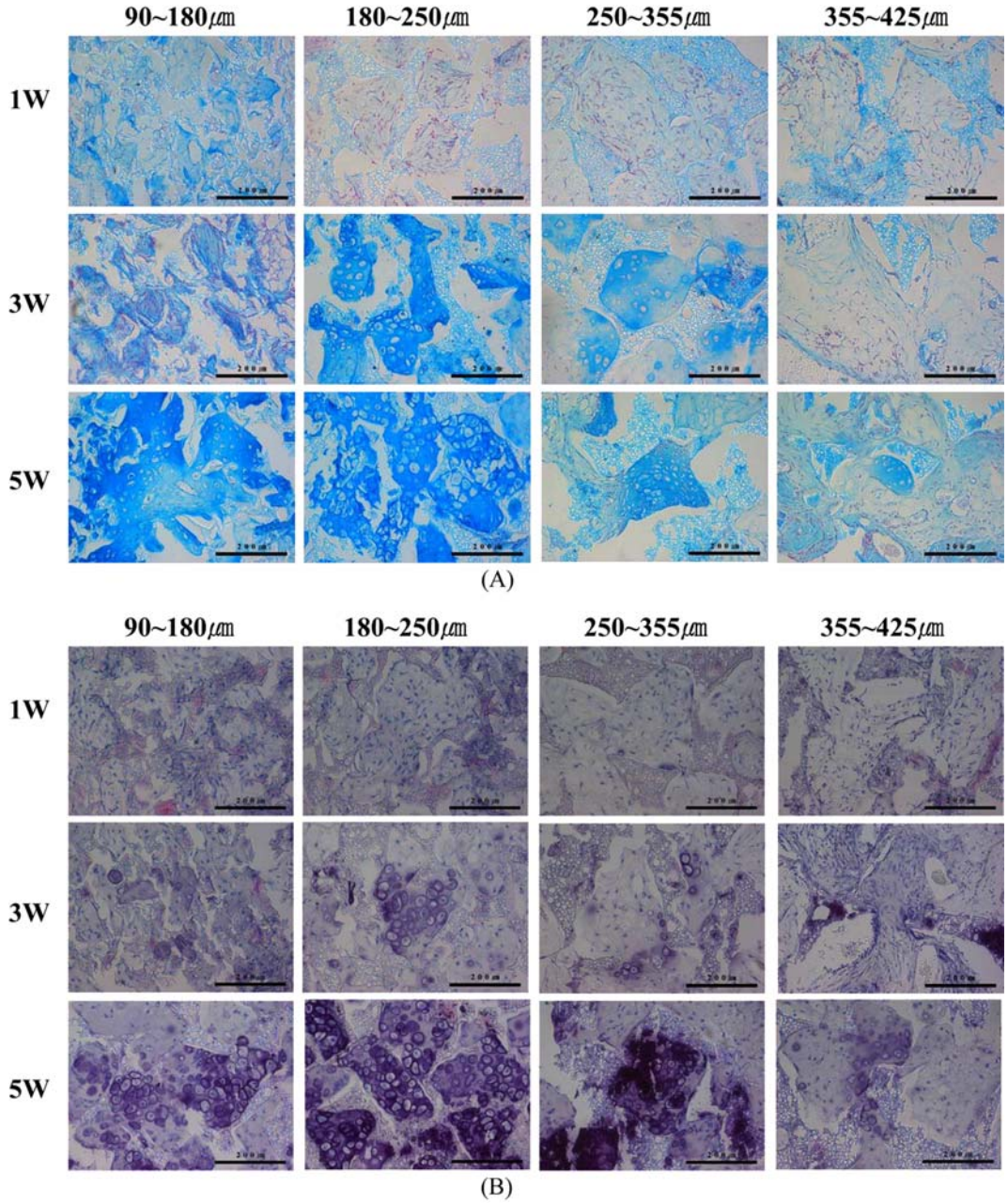

Figure 7. Stained images of chondrocytes on silk fibroin scaffolds at 1, 3, and 5 weeks. (A) Alcian blue and (B) H & E.

expression observed at the peak by week 3. Therefore, RT-PCR results also confirmed that cell attachment and proliferation were most efficient for scaffolds with 90-250 μm pores, consistent with the formation of abundant extracellular matrix components.

Histological Evaluation and Analysis. To confirm the adhesion and proliferation of chondrocytes on scaffolds with various pore sizes, we used histological analysis with alcian blue (Figure 7(A)) and H&E staining (Figure 7(B)) after 1, 3, and 5 weeks of cells growth. As shown in Figure 7(A), alcian blue staining demonstrated that the number of chondrocytes increased from 1 to 3 weeks of culture. Cell adhesion was observed on the scaffold after 1 week, but the formation of lacunae was not observed. However, lacunae were observable by 3 weeks of culture and were quite obvious by week 5. In H&E-stained samples, lacunae of chondrocytes were not observed until 5 weeks of culture. Based on the histological analysis, scaffolds with pore sizes of 180-250 μm exhibited the most lacunae of chondrocytes. Hence, the resulting 180-250 μm pore permeability of our as-fabricated scaffold indicates efficient oxygen and nutrient supply which in turn helps the growth of chondrocytes and provides favorable environment for the culture

of chondrocytes.

Conclusions

In conclusion, silk fibroin scaffolds with various pores sizes (*i.e*. 90-180, 180-250, 250-355, and 355-425 μm) were used to study the adhesion and proliferation of chondrocytes. All the scaffolds was fabricated *via* salt extraction method followed by its physiochemical and mechanical properties analysis including FTIR, comprehensive strength, etc. Results showed that the mechanical strength decreased as the pore size increased. Importantly, better cell adhesion and proliferation were observed in scaffolds with smaller pore sizes, which also exhibited highest levels of sGAG, collagen, aggrecan, and type II collagen. Thus it can be concluded that silk fibroin scaffolds having 90-250 μm pores size provided the optimal environment for cartilage cell adhesion and proliferation. However, further detailed studies are required to determine the potential applications of silk scaffold in tissue engineering and regenerative medicine especially for cell division and differentiation of chondrocytes.

Acknowledgments. This research was supported by Brain Korea 21 PLUS Project, NRF, NRF-2012M3A9C6050204 and Bio-industry Technology Development Program (112007-05-3-SB010), Ministry for Food, Agriculture, Forestry and Fisheries, Republic of Korea.

References

(1) T. H. Qazi, R. Rai, and A. R. Boccaccini, *Biomaterials*, **35**, 9068 (2014).
(2) D. Schumann, A. K. Ekaputra, C. X. Lam, and D. W. Hutmacher, *Methods Mol. Med.*, **140**, 101 (2007).
(3) A. Vats, N. S. Tolley, J. M. Polak, and J. E. Gough, *Clin. Otolaryngol. Allied Sci.*, **28**, 165 (2003).
(4) S. J. Lee, *Int. J. Tissue Regen.*, **4**, 89 (2013) .
(5) S. L. Niemansburg, J. J. van Delden, F. C. Oner, W. J. Dhert, and A. L. Bredenoord, *Spine J.*, **14**, 1029 (2014).
(6) A. French, J. Y. Suh, C. Y. Suh, L. Rubin, R. Barker, K. Bure, B. Reeve, and D. A. Brindley, *Trends Biotechnol.*, **32**, 436 (2014).
(7) A. Atala, *J. Pediatr. Surg*., **47**, 17 (2012).
(8) E. Cosgriff-Hernandez and A. G. Mikos, *Pharm. Res.*, **25**, 2345 (2008).
(9) L. M. Li, M. Han, G. Khang, and J. Q. Gao, *Int. J. Tissue Regen.*, **4**, 65 (2013).
(10) L. P. Yan, J. M. Oliveira, A. L. Oliveira, S. G. Caridade, J. F. Mano, and R. L. Reis, *Acta Biomater.*, **8**, 289 (2012).
(11) S. Talukdar, Q. T. Nguyen, A. C. Chen, R. L. Sah, and S. C. Kundu, *Biomaterials*, **32**, 8927 (2011).
(12) Y. Wang, D. J. Blasioli, H. J. Kim, H. S. Kim, and D. L. Kaplan, *Biomaterials*, **27**, 4434 (2006).
(13) F. J. O'Brien, B. A. Harley, M. A. Waller, I. V. Yannas, L. J. Gibson, and P. J. Prendergast, *Technol. Health Care*, **15**, 3 (2007).
(14) C. M. Murphy, M. G. Haugh, and F. J. O'Brien, *Biomaterials*, **31**, 461 (2010).
(15) C. Lane and J. Boulton, *Adv. Biosci*., **63**, 125 (1987).
(16) G. L. Wilkes and S. L. Samuels, *J. Biomed. Mater. Res*., **7**, 541 (1973).
(17) L. Norton and M. Chvapil, *J. Trauma*, **21**, 463 (1981).
(18) K. J. Quinn, J. M. Courtney, J. H. Evans, J. D. S. Gaylor, and W. H. Reid, *Biomaterials*, **6**, 369 (1985).
(19) P. Le Bail, F. G. Morin, and R. H. Marchessault, *Int. J. Biol. Macromol*., **26**, 193 (1999).
(20) M. K. Yoo, H. Y. Kweon, K. G. Lee, H. C. Lee, and C. S. Cho, *Int. J. Biol. Macromol*., **34**, 263 (2004).
(21) C. Correia, S. Bhumiratana, L. P. Yan, A. L. Oliveira, J. M. Gimble, D. Rockwood, D. L. Kaplan, R. A. Sousa, R. L. Reis, and G. Vunjak-Novakovic, *Acta Biomater.*, **8**, 2483 (2012).
(22) H. S. Park, M. S. Gong, J. H. Park, S. I. Moon, I. B. Wall, H. W. Kim, J. H. Lee, and J. C. Knowles, *Acta Biomater.*, **9**, 8962 (2013).
(23) Y. Wang, D. D. Rudym, A. Walsh, L. Abrahamsen, H. J. Kim, H. S. Kim, C. Kirker-Head, and D. L. Kaplan, *Biomaterials*, **29**, 3415 (2008).
(24) J. Jin, J. Wang, J. Huang, F. Huang, J. Fu, X. Yang, and Z. Miao, *J. Biosci. Bioeng.*, **118**, 593 (2014).
(25) B. Kundu, R. Rajkhowa, S.C. Kundu, and X. Wang, *Adv. Drug Deliv. Rev.*, **65**, 457 (2013).
(26) M. Demoor, D. Ollitrault, T. Gomez-Leduc, M. Bouyoucef, M. Hervieu, H. Fabre, J. Lafont, J. M. Denoix, F. Audigie, F. Mallein-Gerin, F. Legendre, and P. Galera, *Biochim. Biophys. Acta*, **1840**, 2414 (2014).
(27) Q. Han, L. Fan, B. C. Heng, and Z. Ge, *Int. J. Tissue Regen.*, **4**, 61 (2013).
(28) E. G. Khaled, M. Saleh, and S. Hindocha, *Open Orthop. J.*, **5**, 289 (2011).
(29) Yannas IV, *Clin. Mater*., **9**, 179 (1992).
(30) Q. Zhang, H. Lu, N. Kawazoe, and G. Chen, *Acta Biomater.*, **10**, 2005 (2014).
(31) T. A. Kelly, B. L. Roach, Z. D. Weidner, C. R. Mackenzie-Smith, G. D. O'Connell, E. G. Lima, A. M. Stoker, J. L. Cook, G. A. Ateshian, and C. T. Hung, *J. Biomech.*, **46**, 1784 (2013).
(32) Y. Zhang, C. Wu, T. Friis, and Y. Xiao, *Biomaterials*, **31**, 2848 (2010).